NANO LETTERS

2008
Vol. 8, No. 8
2410-2418

Plasmon Field Effects on the Nonradiative Relaxation of Hot Electrons in an Electronically Quantized System: CdTe−Au Core−Shell Nanowires

Svetlana Neretina,[†] Wei Qian,[†] Erik Dreaden,[†] Mostafa A. El-Sayed,*[,†] Robert A. Hughes,[‡] John S. Preston,[‡,§] and Peter Mascher[§]

Laser Dynamic Laboratory, School of Chemistry and Biochemistry, Georgia Institute of Technology, Atlanta, Georgia 30332-0400, Brockhouse Institute for Materials Research, McMaster University, Hamilton, Ontario, L8S 4M1, Canada, and Department of Engineering Physics, McMaster University, Hamilton, Ontario, L8S 4L7, Canada

Received May 6, 2008; Revised Manuscript Received June 1, 2008

ABSTRACT

The intense electromagnetic fields of plasmonic nanoparticles, resulting from the excitation of their localized surface plasmon oscillations, are known to enhance radiative processes. Their effect on the nonradiative electronic processes, however, is not as well-documented. Here, we report on the enhancement of the nonradiative electronic relaxation rates in CdTe nanowires upon the addition of a thin gold nanoshell, especially at excitation energies overlapping with those of the surface plasmon oscillations. Some possible mechanisms by which localized surface plasmon fields can enhance nonradiative relaxation processes of any quantized electronic excitations are proposed.

The phenomenon of localized surface plasmon resonance (LSPR) was first treated by Gustav Mie in 1908.[1] It was observed that, when resonant light interacts with noble metal nanoparticles, it gives rise to collective oscillations of their conduction electrons. The brilliant colors observed are a result of photon absorption and scattering that occur when these oscillating electrons become resonant with the incident electromagnetic radiation. The strong electromagnetic fields associated with plasmonic nanoparticles, arising from the electromagnetic excitation of their localized surface plasmon (LSP) oscillations,[2−5] have been shown to enhance a number of radiative processes such as absorption,[6,7] fluorescence,[8,9] Mie[10] and Raman scattering.[11,12] The influence of these plasmonic fields on nonradiative processes is, for the most part, undocumented. There do exist, however, a few recent reports illustrating such effects. Included among these are (i) the plasmon-assisted Förster energy transfer of dye molecules and silver nanoparticles, which has been studied both experimentally[13] and theoretically,[14] (ii) the theoretical study of the plasmon-enhanced Förster energy transfer between semiconducting nanoparticles,[15] (iii) the measured period of the coherent lattice oscillations of gold nanoparticles being found to increase in the presence of localized surface plasmon fields,[16] and (iv) the observation that the plasmonic fields from gold nanoparticles change the rate of the subpicosecond retinal photoisomerization in bacteriorhodopsin (bR), the only other photosynthetic system found in nature besides chlorophyll.[17]

The current interest in nanostructure fabrication has provided the opportunity to study the influence that these plasmonic fields have on both the radiative and the nonradiative properties of quantum confined systems. The radiative phenomenon of fluorescence is well-known to be enhanced. The effect was elegantly demonstrated by Lee et al.[18] in the core−shell CdTe nanowire system present in a colloidal solution. It was shown that, if a 5 nm thick protein layer was used to separate CdTe from the gold nanoshell, thereby eliminating the efficient energy and/or electron transfer quenching mechanisms, then a large fluorescence yield enhancement was observed due to the proximity to the plasmonic field.

An investigation of the influence of a gold nanoshell on the electronic nonradiative relaxation processes requires a system where the gold atoms are in intimate contact with the material being investigated, negating any possibility of interference from a capping material. It is difficult to establish

* Corresponding author. E-mail: melsayed@gatech.edu. Phone: 404-894-0292.
[†] Georgia Institute of Technology.
[‡] Brockhouse Institute for Materials Research, McMaster University.
[§] Department of Engineering Physics, McMaster University.

10.1021/nl801303g CCC: $40.75
Published on Web 06/26/2008

unequivocally if such a requirement is met for nanowires derived from colloidal preparations. In this communication, we have thus examined the effect that plasmonic fields have on the nonradiative electronic relaxation rates of hot electrons in CdTe nanowires (width = 75, height = 200 nm) coated with a 15 nm gold nanoshell. The observed response can be described in terms of two proposed mechanisms. The first is an energy and/or electron transfer process that allows for the cooling of the hot electrons having energies different from that of the localized surface plasmons. The second mechanism describes the role of plasmonic fields in the cooling of hot electrons having excited energies that overlap with those of the localized surface plasmons in the gold nanoshell. In this case, an additional highly efficient relaxation process is observed when the hot electrons in CdTe and the localized surface plasmons of gold are simultaneously excited. The report is concluded with a qualitative discussion describing some of the possible mechanisms by which a plasmonic near-field can enhance the nonradiative relaxation in any quantized electronically excited system, such as electronically excited molecules, ionic solids, or biological systems.

Sample Preparation. The CdTe nanowire samples used in this work were derived from the catalytically driven vapor−liquid−solid growth mode.[19] The growth process required an initial deposition of a bismuth film onto a surface corrupted [0001] sapphire substrate that, when heated to sufficient temperatures, would dewet to form nanometer scale catalytic seeds.[20] When exposed to a flux of cadmium and tellurium atoms, produced using the pulsed lased deposition technique (PLD), these seeds initiated a one-dimensional growth mode that results in the formation of CdTe nanowires. Of note is the fact that these nanowires grow in the absence of a two-dimensional planar layer, a feature that usually accompanies the growth of other semiconductor nanowire systems. Further details regarding the deposition process can be found elsewhere.[20,21]

The produced CdTe nanowires are vertically aligned and share an epitaxial relationship with the substrate. The nanowire sidewalls are highly faceted, showing a hexagonal geometry when viewed from above. Typical nanowire widths and heights, for the sample that is the primary focus of the work presented here, are 75 and 200 nm, respectively. Figure 1 shows an SEM image of these nanowires. X-ray diffraction measurements indicate that the CdTe nanowires exist in the wurtzite crystal structure instead of the zinc blende structure normally associated with the bulk material.[17] TEM measurements show a pure wurtzite phase with no evidence of the parasitic zinc blende phase commonly observed in wurtzite GaAs nanowires.[22] Of significance to this work is that there exists across the surface of the substrate a symmetric nanowire density distribution with the center of the substrate having the highest density of nanowires and the edges showing the lowest density. Subsequent to growth, a 15 nm film of gold was sputtered onto one-half of the sample such that one side of the symmetric distribution of nanowire densities consisted of CdTe nanowires while the other consisted of CdTe−Au core−shell nanowires.

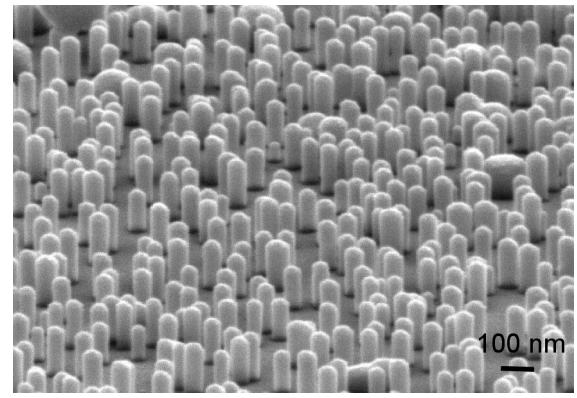

Figure 1. SEM image of the Au-coated CdTe nanowires used in this study. Samples were synthesized by the catalytically driven vapor−liquid−solid growth mode. Typical nanowire widths and heights are 75 and 200 nm, respectively.

Microabsorption Spectroscopy. Microabsorption spectra, obtained using an SEE 1100 microspectrometer, were recorded at various points across the CdTe nanowire density gradient for both the gold coated and the uncoated portions of the sample. Each spectrum was obtained from a 3.75 μm diameter area using a 50× objective. The spectral response for wavelengths ranging from 400 to 900 nm was recorded to a 3 nm resolution using a 600 lines/mm diffraction grating in combination with a charge coupled device (CCD) detector. The measurements were taken using unpolarized light with a propagation direction parallel to the axial length of nanowires (i.e., along the dimension normal to the substrate).

Figure 2 shows a plot of the extinction spectra obtained for various CdTe nanowire densities both in the absence (Figure 2a) and in the presence (Figure 2b) of a 15 nm thick gold nanoshell. The extinction spectra for the uncoated nanowires, shown in Figure 2a, have two distinct features: (i) a band edge at 770 nm and (ii) a broad extinction band in the 400−500 nm region due to the overlapping interband transitions. The CdTe band edge is similar to that observed for bulk wurtzite CdTe,[23] as is expected for wire dimensions that are much larger than the 7.5 nm exciton Bohr radius in CdTe. Of note is that similar features are observed for zinc blende CdTe films produced from the same target. Thus, it is likely that the spectra shown are close to those expected for the bulk wurtzite phase. This, however, is not easily verified as the bulk wurtzite phase is difficult to synthesize.[24] Also of significance is the spectral response of the broad extinction band as the density of the nanowires is varied. As expected, the extinction increases as the density of nanowires increases. Surprising, however, is the red shift of the strong band maximum in the 400−500 nm region with increasing nanowire density. This could result from the coupling between the transition moments of this strong absorption in adjacent nanowires.

Figure 2b shows data similar to that shown in Figure 2a except, in this case, the spectral response is that from CdTe nanowires with a gold nanoshell. The extinction spectra for these core−shell nanowires exhibit the same features present in the uncoated nanowires, but with two added features: (i) a shoulder at the long wavelength side of the 400−500 nm

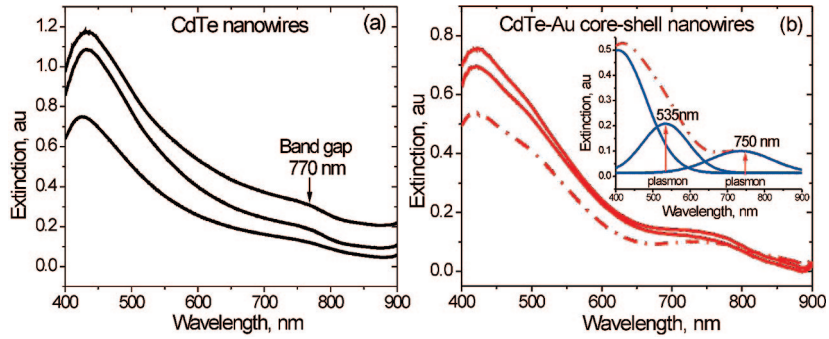

Figure 2. Extinction spectra of (a) uncoated CdTe nanowires and (b) CdTe−Au core−shell nanowires. The three spectra shown in each graph correspond to various nanowire densities, where the magnitude of the extinction at short wavelengths increases as the nanowire density increases. The inset to b shows the deconvolution of the low intensity spectrum (dashed-dotted curve) using three Gaussians. The increased absorptions near 530 and 750 nm, observed when the gold nanoshell is added, are assigned to the localized surface plasmon absorption.

peak that is especially noticeable at lower nanowire densities, and (ii) a broad shoulder in the 750 nm region, which overlaps with the band edge absorption. As is shown in the inset to Figure 2b, we were able to deconvolute the core−shell spectra (dashed-dotted curve) using only three Gaussians. The peaks centered at 530 and 750 nm do not exhibit any apparent distortion due to the CdTe extinction in these regions. It is possible that the weaker CdTe extinctions in these regions are overwhelmed by the stronger plasmon extinction and/or by the fact that CdTe extinctions in these regions get the expected plasmon field enhancement that gives them a profile similar to the surface plasmon band shapes. The rise in the extinction spectrum below 500 nm is due to the interband absorption of CdTe with an additional contribution likely originating from the interband absorption of metallic gold (see prediction of the discrete dipole approximation (DDA) calculations in the next section). For the high density of core−shell structures, there appears to be a spectral distortion of the 750 nm plasmon peak. Such a distortion could result from a red shift of the surface plasmon band due to a coupling between the surface plasmon dipoles facilitated by high nanowire densities. This would then allow for the observed band edge profile. These conclusions are supported by the DDA calculations, described in the next section, which were used to generate the expected spectra for a gold shell in the presence of the dielectric constant of CdTe.

DDA Calculations for the CdTe−Au Core−Shell Nanowires. Optical extinction properties of the CdTe−Au core−shell nanostructures were calculated by discrete dipole approximation (DDA).[25,26] DDA is a well-established finite element method of computational electrodynamics used to numerically derive optical responses to electromagnetic fields for particles of arbitrary size, shape, composition, and environment. Due to its ability to accurately account for the effects of optical retardation and multipolar localized surface plasmon resonance, DDA has become a versatile, yet powerful, tool in studying the optical properties of plasmonic nanostructures.[27–34] Briefly, the target particle is described as a cubic array of point dipoles, to each of which is assigned a discrete dielectric function and dielectric environment. The polarizability of each element in the array is then formulated by the lattice dispersion relation[35,36] and their $3N \times 3N$ dipole interaction matrix is generated. The total electric field, which represents the superposition of the incident plane wave and the fields radiating from surrounding dipoles, is then used to iteratively calculate the polarization at each point in the array. Fortran codes developed by Draine and Flatau[37] utilize fast Fourier transform methods to perform the former and complex conjugate gradient techniques to perform the latter. Once the polarization at each point in the array is determined, the optical extinction properties of the particle are directly calculated.[38]

Here, optical extinction spectra were simulated using the experimentally derived complex refractive indices for Au provided by Johnson and Christy,[39] and for CdTe provided by Palik.[40] DDA calculations were performed for nanowires whose dimensions most accurately reflect those of the experimental sample using mean size parameters for the CdTe nanowires as determined by scanning electron microscopy and an Au film thickness obtained from tapping-mode atomic force microscopy. In this case, the DDA calculations were performed for a hemispherically capped, cylindrical CdTe core, 183.85 nm in length and 73.55 nm in diameter, with a fixed Au shell thickness of 14.7 nm and a total of 61 397 point dipoles. The incident plane wave was chosen to propagate along the longitudinal axis of the core with a fixed orthogonal polarization and an in vacuo environment.

Figure 3 shows the size-normalized extinction, absorption, and scattering spectra calculated for these CdTe−Au core−shell nanowires. It can be seen that the spectra are characterized by at least three peaks: (i) an intense shoulder in the 500 nm region, (ii) a weak band in the 750 nm region, and (iii) a moderately intense band in the 900 nm region. The fast rise in the spectra below 500 nm is due to the interband absorption of metallic gold. The results of the DDA calculations confirm the presence of two plasmon bands in the spectral region covered by the microabsorption measurements, one in the 500 nm region and the other in the low energy region near the band edge absorption. These calculations support our earlier conclusion made through a comparison of the extinction spectra of CdTe to that of the CdTe−Au core−shell structure (Figure 2b).

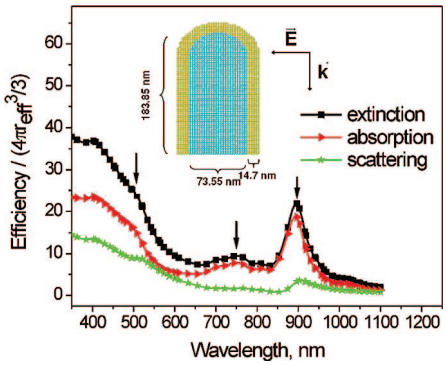

Figure 3. Size-normalized DDA simulations for CdTe−Au core−shell nanostructures. Calculations were performed for a hemispherically capped, cylindrical CdTe core, 183.85 nm in length and 73.55 nm in diameter, with a Au shell thickness of 14.7 nm and a total of 61 397 point dipoles. The incident plane wave was chosen to propagate parallel to the longitudinal axis of the particle, with a fixed orthogonal polarization and an in vacuo environment.

Electron Dynamics in CdTe−Au Core−shell Nanostructures. Femtosecond pump−probe studies were used to assess the hot electron carrier dynamics in these nanostructures at room temperature. These time-resolved optical techniques have become powerful tools in the study of charge carrier dynamics and electronic structures in a broad range of materials that include both bulk materials and nanostructures.[41,42] The laser system used for these measurements is described in detail elsewhere[43] and will only be described briefly here. An amplified Ti−sapphire laser system (Clark MXR CPA 1000) is pumped by a frequency-doubled Nd:vanadate laser (Coherent Verdi) to obtain 800 nm laser pulses that are of 100 fs in duration (fwhm) having an energy of 1 mJ and a repetition rate of 1 kHz. These pulses are then frequency doubled using a BBO crystal to create 400 nm pump pulses. While the majority of this pulse is used to pump the sample, a small portion ($E \approx 40\ \mu$J) is passed through a sapphire plate, generating a femtosecond white light continuum ($\lambda = 400$ to 1100 nm) to be used as the probe beam. The pump beam travels through a variable optical delay line (3 μm resolution) and is passed through a HMS221 synchronous mechanical light beam chopper ($f = 492$ Hz), where a master clock (Clark-MXR DT 505) is used to set the frequency and phase of the chopper. The pump and probe beams are then focused onto the sample (spot size diameter $= 250\ \mu$m) such that there is complete spatial overlap and variable temporal overlap. Noise, due to fluctuations in the white light continuum, is minimized using a reference beam that is split off from the probe beam before it reaches the sample. Both the reference and the transmitted beams are focused onto fiber optics coupled to a monochromator (Acton Research). After passing through the monochromator, the two beams are detected by two matched photodiode (Thorlabs), boxcar integrator (Stanford Research System, SR 250) systems. The output from the signal boxcar is then divided by the output from the reference boxcar using an analog divider. Single wavelength kinetics and transient absorption spectra ranging from 450 to 750 nm were monitored using a monochromator/photodiode arrangement coupled to a boxcar integrator and a lock-in amplifier (Stanford Research System SR 530). This amplifier monitors the output from the analog divider using the signal from the mechanical chopper as its reference frequency. The induced changes in the sample's absorption are then probed by measuring the differential transmission, given by $\Delta T(t)/T = (T_{on}(t) - T_{off})/T_{off} = -\Delta\alpha(t)L$, as a function of the temporal delay between the pump and the probe. Here, T_{on} and T_{off} refer to the transmission with and without the pump beam, and L is the interaction length between the pump (or probe) pulse and the sample. The high stability of the femtosecond laser system as well as the phase-lock technique permits high sensitivity measurements with a $\Delta T/T$ noise level in the 10^{-4} range. The cross-correlation between the pump beam and the visible probe beam has a fwhm of 160−180 fs at the sample position.

Figure 4A shows a plot of the transient bleaching versus the delay time for probe wavelengths of 770, 700, 650, and 550 nm. For both the nanowire and the core−shell structures, the hot electron lifetime decreases as the energy of the incident photon increases. For the uncoated nanowires, the observed lifetimes are 4.5, 2.1, 1.3, and 0.8 ps for probe wavelengths of 770, 700, 650, and 550 nm, respectively. For the core−shell structures, the lifetimes at the same probe wavelengths are 2.5, 1.5, 1.1, and 0.4 ps. The observed decrease in hot electron lifetimes with increasing probe energies for both the nanowires and the core−shell structures is not surprising as it is expected from Fermi's Golden Rule. As the energy of the excited-state increases, so too does the density of the accepting electron−phonon (sink) modes. For the 770 nm probe wavelength, the excited electrons are in the band gap state and are only able to relax either by giving their energy to phonons or by impurity scattering processes. With decreasing probe wavelength, however, the electrons are excited to higher energy states and are hence able to relax through intraband transitions. The higher the energy, the larger the role that these intraband transitions play in the relaxation of the hot electrons, thus increasing the number of the accessible energy states.

The above explanation is equally applicable to the core−shell nanostructures as it is to the uncoated nanowires. In the core−shell system, however, new mechanisms become possible due to the presence of the additional electronic systems of gold. It is for this reason that, for all probe wavelengths, the relaxation process from these excited states is faster for the core−shell structures than it is for the uncoated nanowires. The induced relaxation by the gold nanoshell could involve energy and/or electron transfer processes. In the energy transfer process, the added electronic states of the gold system offer new relaxation pathways, thus increasing the relaxation rate. In addition, there exists a new mechanism that becomes important when the excitation in the semiconductor is resonant with the plasmonic energy. In this scenario, strong exciton−plasmon Coulombic coupling leads to a rapid annihilation of the exciton and the creation of the plasmon (Figure 5). Such a process gives rise to the nonradiative decay of excitons (i.e., the relaxation of excited states). The only requirement for the occurrence of

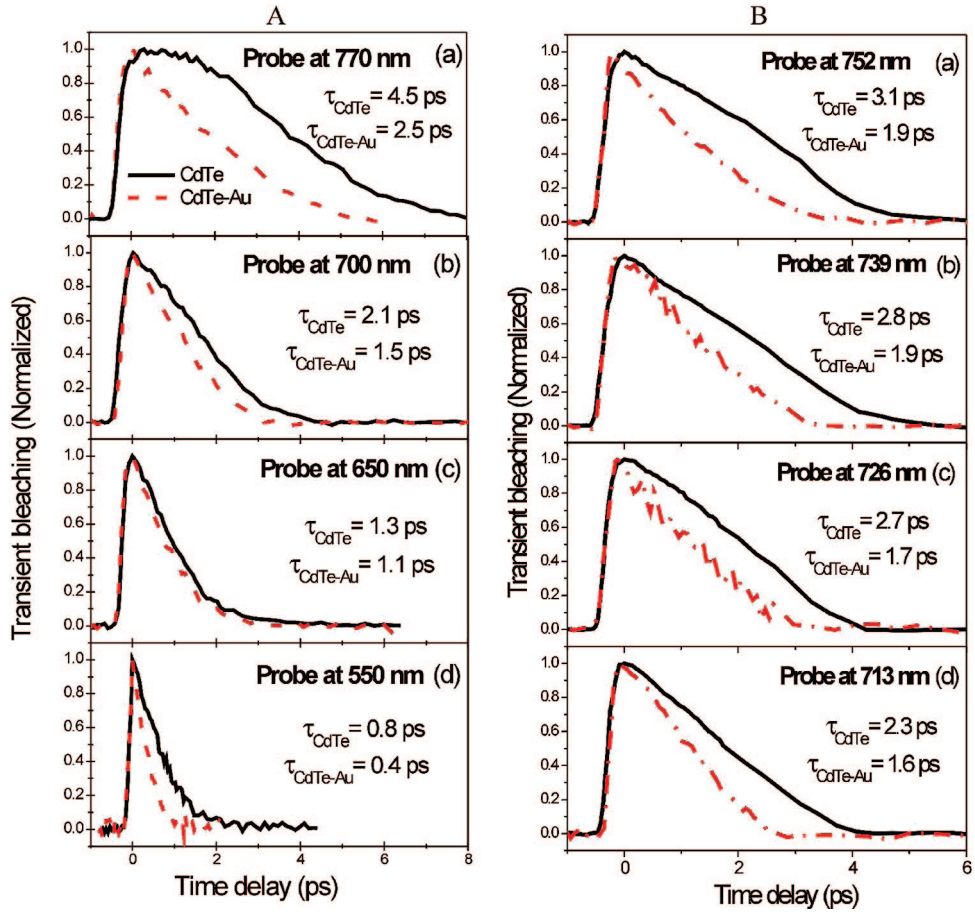

Figure 4. Plots showing the transient bleach intensity as a function of the delay time for the probe wavelengths of (A) 770, 700, 650, 550 nm and (B) 752, 739, 726, 713 nm. The response shown originates from the excitation and subsequent decay of electrons in the nanostructures under study. The solid lines show the decays from uncoated CdTe nanowires while the dashed lines show the decays from the CdTe−Au core−shell nanowires.

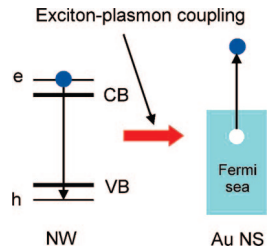

Figure 5. Schematic illustrating the mechanism where an exciton in the semiconductor nanowire system (NW) is annihilated to form a surface plasmon oscillation in the gold nanoshell (Au NS) due to the Coulombic interaction. This process could contribute to the cooling of hot electrons in the CdTe NW for energies able to excite a surface plasmon in the gold nanoshell. Such a process would contribute to the rapid decay of the excited states (i.e., the exciton) in the semiconducting nanowire when in close proximity to the gold plasmon system.

this mechanism is that the excited state must decay to a state whose energy is lower by an amount equal to surface plasmon energy. This process should be quite effective in quenching the band gap emission when the emission energy is in resonance with the surface plasmon absorption. The relatively long radiative lifetime of the band gap state, due to the absence of the nonradiative intraband relaxation processes, makes such exciton−plasmon coupling highly probable.

In the electron transfer mechanism, there is a transfer of an excited electron in the semiconductor's conduction band to the conduction band of the gold nanoshell. Previous calculations indicate that the Fermi level of the gold nanoshell is located below the excited level of the CdTe semiconductor.[44] It is expected that this transfer would be accompanied by an electron transfer from the valence band of the gold to the semiconductor in order to neutralize its excited hole.

Of great importance to this work is the fact that the difference in relaxation times between the CdTe nanowires and the CdTe−Au core−shell structures progressively decreases for the probe wavelengths of 770, 700, and 650 nm, but then increases for the 550 nm monitoring wavelength. The initial decrease is expected as the higher energy excitations are able to relax through intraband transitions, reducing the importance of relaxation processes utilizing the gold system. The reversal at 550 nm, however, was not expected and provides strong evidence for the existence of an additional efficient relaxation process in the core−shell structures. This effect is also made obvious by plotting the relaxation rate constants of the decays (the inverse of the decay time) against the probe wavelength. The results, shown in Figure 6, clearly show a divergence between the two sets

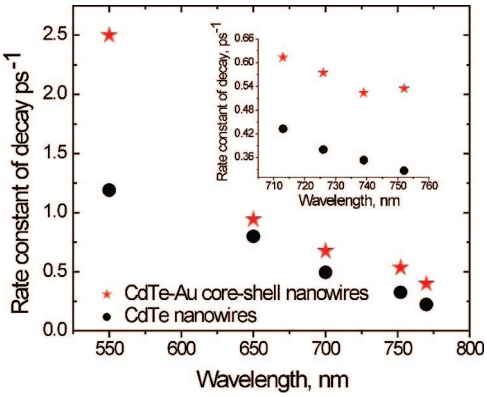

Figure 6. Hot electron relaxation rate constants for CdTe nanowires (●) and CdTe−Au core−shell nanowires (★) as a function of the probe wavelength. The divergence in the data for probe wavelengths coincident with the 550 and 750 nm (see inset) plasmon absorption peaks is consistent with the presence of a new relaxation mechanism that is closely associated with the surface plasmon field effect of the gold nanoshell.

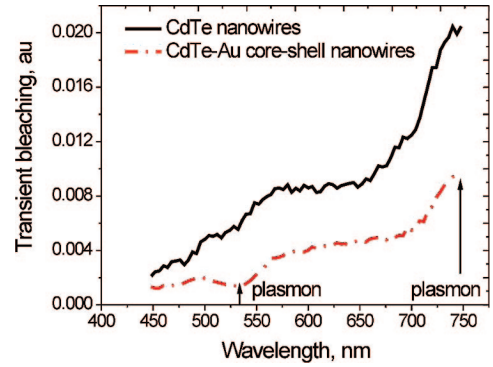

Figure 7. Transient bleach spectra for uncoated CdTe nanowires (solid line) and CdTe−Au core−shell structures (broken line). Note that the two curves run approximately parallel, but diverge near the 530 and 750 nm due to the rapid relaxation of the hot electrons at the precise wavelength associated with plasmon peaks of the gold nanoshell.

of data at the 550 nm probe wavelength, a wavelength which coincides with the 530 nm localized surface plasmon oscillation absorption of gold.

Two possible mechanisms can account for the observed increase in the relaxation rate in the 550 nm region. The first possibility is that the pump pulse at 400 nm induces the bleach in the surface plasmon absorption of the gold shell near this wavelength. In this scenario, the rapid relaxation is not due to the intraband excitations of CdTe electrons but instead is attributed to the electron−phonon relaxation processes associated with just the surface plasmon electronic excitations of Au. The second possibility is that hot electrons in the CdTe nanowires have an enhanced relaxation rate when the monitoring light turns on the surface plasmon field having absorption at 550 nm.

There are two experimental results in support of the surface plasmon field enhancement mechanism. First, is the fact that the observed lifetime of 0.4 ps is too short compared with the accepted 1.0 ps value for the surface plasmon bleach relaxation in gold, a value which is independent of both the nanoparticle's shape and the size.[5] More revealing are the results showing the effect of changing the monitoring light intensity on the observed lifetime. A comparison between the observed lifetimes near the absorption at 550 nm for the CdTe nanowires and those for the CdTe−Au core−shell nanostructures shows that, while there is no effect observed in CdTe nanowires, a factor of 2 increase in the monitoring light intensity gives rise to a 30% increase in the core−shell relaxation rate. The increase observed for the core−shell structure likely originates from an increase of the plasmon field intensity, which in turn, increases the plasmon field enhancement effect on the relaxation rate. It is important to note, however, that no such increase is expected for the first mechanism where the observed decay is attributed to the electron−phonon relaxation processes in the gold shell. In this case, a decrease rather than an increase in the relaxation rate is expected if the intensity is raised to levels able to increase the electron temperature[5] in the gold shell.

If an enhanced relaxation process is associated with the 530 nm plasmon, then it stands to reason that there must exist a similar enhancement for the 750 nm plasmon. In order to investigate this possibility, the decays of the transient bleach intensity in this region were determined and are shown in Figure 4B at 752, 739, 726, and 713 nm. As is expected from Fermi's Golden Rule, there exists a decrease in the observed decays for the uncoated CdTe nanowires as the wavelength decreases. For the CdTe−Au core−shell nanowires, however, the decay lifetime at 752 nm is actually shorter than that observed at 739 nm, once again showing an enhancement in the relaxation rate when in the presence of a surface plasmon field, in this case, at 750 nm (see the inset in Figure 6).

Corroborative support for this surface plasmon induced relaxation process can be seen in the transient bleach spectra (Figure 7). The spectra were obtained using a 400 nm pump to excite electrons while measuring the intensity of the monitoring light at different wavelengths for a fixed time delay of 1 ps. The transient bleach intensity, which is a measure of the difference between the pulsed monitoring light intensity after and that before the 400 nm excitation pulse, is then recorded for each wavelength. The resulting spectrum gives a measure of the hot electron relaxation rate as a function of the excited-state energy, with low transient bleaching intensities corresponding to short-lived states and high intensities corresponding to long-lived states. As expected, the bleach intensity for the CdTe nanowires is higher than that found for the CdTe−Au core−shell nanostructures for all measured wavelengths. As previously discussed, this is a consequence of the additional relaxation processes involving energy and/or electron transfer processes due to the gold electronic system. It should be noted that the two curves run almost parallel to each other over most of the wavelength range with notable exceptions occurring in the 500−570 and 750 nm regions. Here, there exist substantial differences between the spectral intensities. Striking is the fact that these two wavelength regions are coincident with the excitation wavelength of the localized surface plasmons observed for the gold shell.

Summary of Results. The optical measurements performed on uncoated wurtzite CdTe nanowires show a response similar to what we observe for bulk zinc blende films. This is not that surprising since both phases have similar band gaps[45] and were produced from the same PLD target. The relatively large size of the nanowires compared with the Bohr radius for CdTe accounts for the fact that their optical properties are not altered by quantum confinement effects. The microabsorption spectra for the CdTe nanowires have features similar to those observed in zinc blende films derived from the same target. It is, however, noted that the broad peak in the 400−500 nm range red shifts as the nanowire density increases, an effect that could originate from the coupling between the large transition moments in adjacent nanowires. CdTe nanowires exposed to transient pump−probe measurements show a hot electron relaxation rate that increases as the probe energy is increased, a result consistent with Fermi's Golden Rule and one that is commonly observed in other semiconductor nanoparticle systems.[46]

The microabsorption measurements on CdTe−Au core−shell structures show several features not found in the uncoated nanowires. DDA methods were used to model the expected behavior for these core−shell structures and yielded results in good agreement with the experimentally observed spectra. The pump−probe results indicated that the hot electron relaxation times in the CdTe nanowire were strongly influenced by the gold nanoshell. The results for all but the 550 and 750 nm probe wavelengths were as expected and seemed to indicate that the faster relaxation of hot electrons depended more on the gold nanoshell than it did on the density of states of the CdTe system. The lifetime reduction was attributed to the energy and electron transfer pathways as well as an exciton−plasmon coupling mechanism made available by the gold nanoshell. The calculations of Andreev et al.[41] demonstrate that electron transfer pathways are possible for this system since the excited electron states in CdTe are shown to be above the Fermi level of the gold nanoshell. Thus, an efficient relaxation mechanism for the interband and intraband excitations of the CdTe nanowire becomes possible via an electron transfer process from the excited states of CdTe to the gold conduction band. This process is accompanied by the simultaneous transfer of an electron from the gold valence band to the CdTe valence band which neutralizes the hole created by the initial excitation of the semiconductor. In addition, when the exciton energy in CdTe is resonant with the surface plasmon energy, the annihilation of the exciton (i.e., the relaxation of the hot electron) can result in the creation of a surface plasmon in the gold nanoshell.

The results for the two anomalous probe wavelengths (λ = 550 and 750 nm) showed an enhancement in the relaxation rate. The enhancement was also observed as an obvious divergence between the bleach spectra of the CdTe and those of the CdTe−Au nanostructures for these two spectral regions. DDA calculations for the core−shell structure predict the existence of a localized surface plasmon in these wavelength regions, as well as the observed increase in the relaxation rate with increasing monitoring light intensity. Taken together, these facts provide a compelling argument that it is the fields, arising from the excitation of the surface plasmon oscillations through the absorption of the monitoring light, that induce the observed rapid nonradiative relaxation of the excited electrons in the CdTe nanowire.

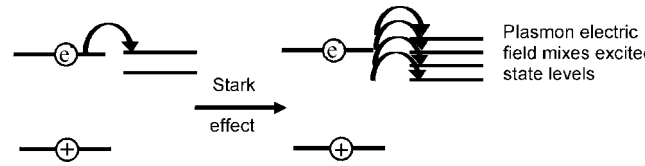

Figure 8. Schematics howing how a Stark-like effect could result in increased nonradiative relaxation pathways. For an excitation in the CdTe system (on the left) there exist a limited number of relaxation pathways. In the presence of a plasmonic field (on the right) an increase in the density of states allows for additional relaxation pathways.

Possible Plasmonic Field Enhancement Mechanisms for Nonradiative Electronic Relaxation Processes. There are two main types of mechanisms that could enhance the nonradiative relaxation of hot electrons in semiconductors or molecules near plasmonic surface fields. In the first mechanism, it is the electric field of the plasmon that alters the energy levels of the semiconductor/gold system. As a result, the energy levels could split and mix in such a manner as to increase the density of the energy accepting states in the semiconductor. Furthermore, the nature of the electronic states themselves could undergo a transformation that could lead to an increase in the electronic coupling between the relaxing and the energy accepting states. For this scenario, the excited electron would relax out of the states being probed to these newly created lower energy states. The second type of mechanism arises from an enhancement of the absorption processes in the semiconductor. The radiative absorption rate for such a process is given by

$$R = |\vec{\mu} \cdot \vec{E}|^2$$

where μ is the transition moment and E is the electromagnetic field strength. The rate of the absorption can thus be enhanced by changing μ, E, or both. Changes to μ occur when there exists an electron transfer between the gold and the semiconductor system or, alternatively, when there exists a mixing of the states by the plasmonic field. This would cause an increase in the transition moment (μ) of the semiconductor transitions in resonance with the surface plasmon energy.

The radiative rate enhancement could also occur if the absorption rate of the monitoring light is enhanced by the gold nanoshell by first capturing a photon to form a surface plasmon. This capture leads to a large increase (or focusing) of the electromagnetic field (E) of the photon being absorbed. Below, we demonstrate the different means by which these mechanisms could arise from the presence of plasmonic fields which, in turn, lead to an enhancement in the rates of nonradiative processes for a semiconductor system having transition energies resonant with those of the surface plasmon.

A. Direct Enhancement of the Nonradiative Process: Stark Effect Mechanism. Stark fields are known to split

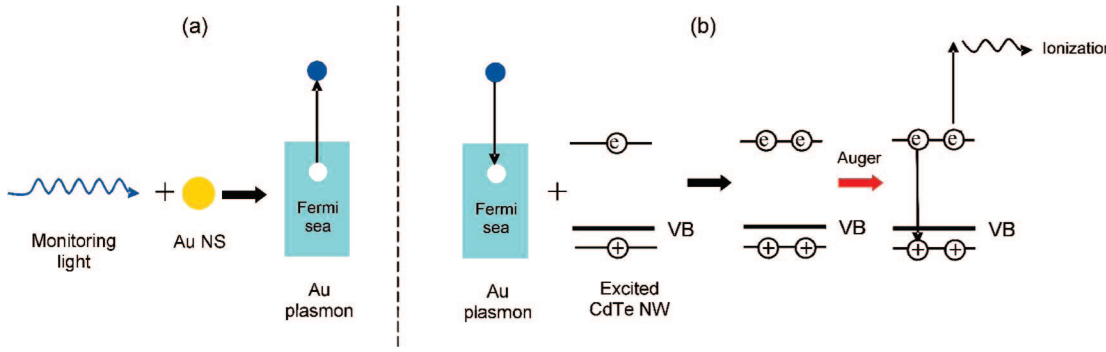

Figure 9. Schematic illustrating the mode by which enhancements to Auger processes, brought on by the creation of plasmons, lead to the nonradiative relaxation of hot electrons. Initially a focusing effect arises from the absorption of the monitoring light by the Au nanoshell (NS) which leads to plasmon formation (a). This is then followed by a release of this plasmon energy which produces a new electron−hole pair in the CdTe nanowire (b). It is the annihilation of two electron−hole pairs in the Auger process, where one electron−hole pair recombines while the other is excited to a higher energy state through the absorption of the energy of recombination, which leads to the removal of the hot electrons being monitored.

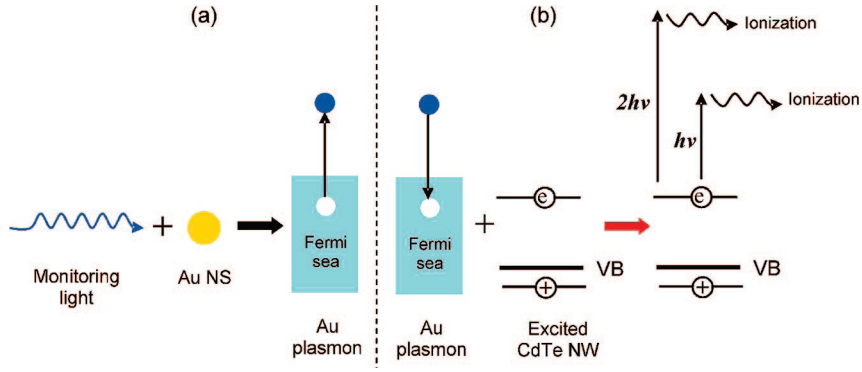

Figure 10. Schematic illustrating how the enhanced absorption to higher dissipative states leads to enhanced nonradiative relaxation of hot electrons in the CdTe nanowire. Initially a focusing effect arises from the absorption of the monitoring light by the Au nanoshell (NS) which leads to plasmon formation (a). This plasmon energy is then transferred to the already hot CdTe electrons promoting them to higher ionization states (b). The net result is to remove excited electrons from the states being monitored.

and mix different electronic or hole states in a semiconductor. This leads to mixing of the wave functions and increases the density of states that can accept the excited-state energy of a hot electron, thus increasing its rate of relaxation. The strong electric field of the electromagnetic plasmonic field could induce Stark excited-state level splitting and mixing, which in turn could lead to an increase in the rate of relaxation of the hot electrons in any electronic quantized system. If the electron−hole semiconductor system is exposed to plasmonic fields (Figure 8), it is possible that these intense fields mix the conduction band states of the CdTe nanowire resulting in an increase in the density of the energy accepting states. Accompanying the increased density of states is an increased number of nonradiative relaxation pathways.

B. Mechanisms Involving the Enhancement of Absorption (Radiative Processes): (I) Auger Mechanism. It is known that Auger processes provide an efficient mechanism for the relaxation of hot electrons in semiconductor nanocrystals due to multiple exciton formation.[47] It is also known that plasmonic gold nanoparticles have a strong radiative probability for the capture of light at resonant energies. The resulting electromagnetic fields are large enough to facilitate the transfer of the plasmon energy to the nearby electronic ground states of the semiconductor due to the strong Coulombic coupling between the plasmon and the excitonic systems. Thus, when the monitoring wavelength is in resonance with the plasmon oscillations and the semiconductor exciton energies, as was the case for the CdTe/Au core−shell system presented here, it becomes highly probable that a second exciton will form. This scenario leads to rapid Auger processes where one of the two excited electron−holes gives up its energy of recombination to the originally excited pair, and it is this ionization of the excited pair that leads to the rapid relaxation of hot electrons (Figure 9).

(II) Enhanced One- or Two-Photon Absorption Mechanism. It is also possible that the strong plasmon field, due to the focusing effects of the absorbed monitoring light by the gold nanoshell, results in enhanced absorption by the CdTe nanowire. This enhancement could give rise to one- or two-photon excitation processes of CdTe's excited state, a process which leads to the ionization of the hot electrons (Figure 10). Thus, the rate of the relaxation for the initially excited hot electron will be enhanced.

In all of the above mechanisms, further excitations occur through changes to the configuration of the electrons. This was done to illustrate the generality of the mechanism when applied to any quantized electronic system such as molecules. In semiconductors, changes to the configuration of the excited

holes could very well have been used to discuss these mechanisms.

Conclusion. A comparison of the nonradiative relaxation of hot electrons in CdTe nanowires to those in CdTe−Au core−shell nanostructures clearly demonstrates an increased relaxation rate due to the nanoshell. These processes were attributed to the energy and/or electron transfer pathways made available by the gold nanoshell. Additional efficient relaxation mechanisms were observed when the energy of the states being probed overlapped with those of the localized surface plasmon oscillations in the gold nanoshell. The resonant energy transfer from the exciton of the semiconductor to form a plasmon in the gold nanoshell is expected to be an efficient relaxation mechanism for the exciton. In addition, it is possible that the plasmon is excited by absorption of the monitoring light. Three possible mechanisms were proposed describing the effect of this plasmon on the relaxation rates. One is a direct nonradiative enhancement mechanism and two result from the enhancement of the radiative processes. While such an effect is of fundamental importance to semiconductor core−shell structures, it should be noted that both the effect and the mechanisms proposed should have equally profound implications to molecular and biological systems as well as to photochemical processes exposed to a plasmon field.

Acknowledgment. M.A.E. would like to thank the DMR Division of NSF (Grant 0138391). S.N. would like to acknowledge the financial support provided by the NSERC postdoctoral fellowship program. The McMaster University group would like to acknowledge Canadian Institute for Advanced Research (CIFAR), the Natural Sciences and Engineering Research Council (NSERC), and the Ontario Research and Development Challenge Fund (ORDCF) under the auspices of the Ontario Photonics Consortium (OPC) for the funding provided and the Canadian Centre for Electron Microscopy (CCEM) for access to their facilities.

References

(1) Mie, G. *Ann. Phys.* **1908**, *25*, 377.
(2) Kreibig, U.; Vollmer, M. *Optical Properties of Metal Clusters*; Springer: Berlin, 1995; Vol. 25.
(3) Bohren, C. F.; Huffman, D. R. *Absorption and Scattering of Light by Small Particles*; Wiley: New York, 1983.
(4) Link, S.; El-Sayed, M. A. *Int. Rev. Phys. Chem.* **2000**, *19*, 409.
(5) Link, S.; El-Sayed, M. A. *Annu. Rev. Phys. Chem.* **2003**, *54*, 331.
(6) Dintinger, J.; Klein, S.; Ebbesen, T. W. *Adv. Mater.* **2006**, *18*, 1267–1270.
(7) Schaadt, D. M.; Feng, B.; Yu, E. T. *Appl. Phys. Lett.* **2005**, *86*, 063106.
(8) Song, J. H.; Atay, T.; Shi, S. F.; Urabe, H.; Nurmikko, A. V. *Nano Lett.* **2005**, *5*, 1557–1561.
(9) Kulakovich, O.; Strekal, N.; Yaroshevich, A.; Maskevich, S.; Gaponenko, S.; Nabiev, I.; Woggon, U.; Artemyev, M. *Nano Lett* **2002**, *2*, 1449–1452.
(10) Popov, O.; Zilbershtein, A.; Davidov, D. *Appl. Phys. Lett.* **2006**, *89*, 191116.
(11) Nie, S. M.; Emery, S. R. *Science* **1997**, *275*, 1102–1106.
(12) Huang, X. H.; El-Sayed, I. H.; Qian, W.; El-Sayed, M. A. *Nano Lett.* **2007**, *7*, 1591–1597.
(13) Lakowitz, J. R. *Anal. Biochem.* **2001**, *298*, 1.
(14) Hua, X. M.; Gersten, J. I.; Nitzan, A. *J. Chem. Phys.* **1985**, *83*, 3650.
(15) Govorov, A. O.; Lee, J.; Kotov, N. A. *Phys. Rev. B* **2007**, *76*, 125308.
(16) Huang, W.; Qian, W.; Jain, P. K.; El-Sayed, M. A. *Nano Lett.* **2007**, *7*, 3227–3234.
(17) Biesso, A.; Qian, W.; El-Sayed, M. A. *J. Am. Chem. Soc.* **2008**, *130*, 3258–3259.
(18) Lee, J.; Govorov, A. O.; Dulka, J.; Kotov, N. A. *Nano Lett.* **2004**, *4*, 2323–2330.
(19) Wagner, R. S.; Ellis, W. C. *Appl. Phys. Lett.* **1964**, *4*, 89–90.
(20) Neretina, S.; Hughes, R. A.; Britten, J. F.; Sochinskii, N. V.; Preston, J. S.; Mascher, P. *Nanotechnology* **2007**, *18*, 275301.
(21) Neretina, S.; Hughes, R. A.; Devenyi, G. A.; Sochinskii, N. V.; Preston, J. S.; Mascher, P. *Nanotechnology* **2008**, *19*, 185601.
(22) Dubrovskii, V. G.; Sibirev, N. V. *Phys. Rev. B* **2008**, *77*, 035414.
(23) Lefebvre, P.; Richard, T.; Allegre, J.; Mathieu, H; Combette-Roos, A.; Granier, W. *Phys. Rev. B* **1996**, *53*, 15440.
(24) Neretina, S.; Mascher, P.; Hughes, R. A.; Braidy, N.; Gong, W. H.; Britten, J. F.; Preston, J. S. *Appl. Phys. Lett.* **2006**, *89*, 133101.
(25) Purcell, E. M.; Pennypacker, Cr. *Astrophys. J.* **1973**, *186*, 705.
(26) Draine, B. T. *Astrophys. J.* **1988**, *333*, 848.
(27) Lee, K. S.; El-Sayed, M. A. *J. Phys. Chem. B* **2005**, *109*, 20331.
(28) Yang, W. H.; Schatz, G. C.; Vanduyne, R. P. *J. Chem. Phys.* **1995**, *103*, 869.
(29) Payne, E. K.; Shuford, K. L.; Park, S.; Schatz, G. C.; Mirkin, C. A. *J. Phys. Chem. B* **2006**, *110*, 2150.
(30) Jain, P. K.; Huang, W. Y.; El-Sayed, M. A. *Nano Lett.* **2007**, *7*, 2080.
(31) Kelly, K. L.; Coronado, E.; Zhao, L. L.; Schatz, G. C. *J. Phys. Chem. B* **2003**, *107*, 668.
(32) Noguez, C. *J. Phys. Chem. C* **2007**, *111*, 3806.
(33) Jain, P. K.; El-Sayed, M. A. *Nano Lett.* **2007**, *7*, 2854.
(34) Hu, M.; Chen, J. Y.; Li, Z. Y.; Au, L.; Hartland, G. V.; Li, X. D.; Marquez, M.; Xia, Y. N. *Chem. Soc. Rev.* **2006**, *35*, 1084.
(35) Draine, B. T.; Goodman, J. *Astrophys. J.* **1993**, *405*, 685.
(36) Draine, B. T.; Flatau, P. J. *J. Opt. Soc. Am. A-Opt. Image Sci. Vis.* **1994**, *11*, 1491.
(37) Draine, B. T.; Flatau, P. J. *DDSCAT 6.1 Scripps Institute of Oceanography*, University of California: San Diego, CA, 2005.
(38) Bohren, C. F.; Huffman, D. R. *Absorption and Scattering of Light by Small Particles*; Wiley: New York, 1983.
(39) Johnson, P. B.; Christy, R. W. *Phys. Rev. B* **1972**, *6*, 4370.
(40) *Handbook of optical constants of solids*; Palik, E. D., Ed.; Academic Press: New York, 1998; Vol. 1.
(41) Shah, J. *Ultrafast Spectroscopy of Semiconductors and Semiconductor Nanostructures*; Springer: Berlin, 1999.
(42) Klimov, V. I.; McBranch, D. W.; Leatherdale, C. A.; Bawendi, M. G. *Phys. Rev. B* **1999**, *60*, 13740–13749.
(43) Schill, A. W.; Gaddis, C. S; Qian, W.; El-Sayed, M. A.; Cai, Y.; Milam, V. T.; Sandhage, K. *Nano Lett.* **2006**, *6*, 1940–1949.
(44) Andreev, A. ; Zajacek, J. *29th International Spring Seminar on Electronics Technology* 2006; Vol. 10−14, pp 2002−205..
(45) *Zahlenwerte und Funktionen aus Naturwissenschaften und Technik*; Landolt-Bornstein, New Series, Group III, Vol. 17b, edited by Madelung, O; Springer: New York, 1982.
(46) Yu, P.; Nedeljkovic, J. M.; Ahrenkiel, P. A.; Ellingson, R. J.; Nozik, A. J. *Nano Lett.* **2004**, *4*, 1089.
(47) Achermann, M; Bartko, A. P.; Hollingsworth, J. A.; Klimov, V. I. *Nat. Phys.* **2006**, *2*, 557.

NL801303G